Mechanistic origins for the accelerated dehydration of ethanol in n-butanol/ethanol mixtures in H-ZSM-5

Arno de Reviere[1,2], An Verberckmoes[1], Maarten Sabbe[1,2*].

[1]*Industrial Catalysis and Adsorption Technology (INCAT), Department of Materials, Textiles and Chemical Engineering, Ghent University, Valentin Vaerwyckweg 1, 9000 Ghent, Belgium.*

[2]*Laboratory for Chemical Technology (LCT), Department of Materials, Textiles and Chemical Engineering, Ghent University, Technologiepark 125, 9052 Ghent, Belgium.*

Supporting information

The H-ZSM-5 framework structure with Pnma symmetry, unit cell composition– $HAlSi_{95}O_{192}$ and unit cell parameters: a = 2047.2 pm, b =2010.9 pm, c = 1357.6 pm, α = 89.97°, β = 89.88°, and γ = 89.99° [1] was used in this study.

(S1) Statistical thermodynamic calculations

Reaction equilibrium coefficients, *K*, for elementary reactions are calculated as:

$$K(T) = \frac{\prod_i Q_i(T)}{\prod_j Q_j(T)} exp(-\frac{\Delta E_r}{RT}) \quad \text{(S1)}$$

where *i* and *j* denote products and reactants respectively. ΔE_r is the change in electronic energy at 0 K (including the zero-point vibrational energy) of the reaction and *Q* the total partition function. The electronic energy from the DFT calculation along with the frequencies obtained from the vibrational analysis are used for the statistical thermodynamic calculation. The total partition function for gas-phase species consists of translational, rotational and vibrational contributions. On the other hand, the surface bound complexes in the zeolite are modeled using either the *immobile* or the *mobile adsorbate* method, based on the vibrational analysis [2]. The *immobile adsorbate* method considers all degrees of freedom of the adsorbed species within the zeolite as frustrated motions, which are described by the harmonic oscillator approximation [3]. This *immobile adsorbate* approach has been applied for all surface–bound complexes except for the physisorbed butenes (1-butene, trans-2-butene and cis-2--butene). These loosely–bound physisorbed butenes are considered as *mobile adsorbates*, which retain certain rotational and translational degrees of freedom [3]. Harmonic frequencies associated with these rotational and translational motions were identified based on visual inspection of frequencies

lower than 100 cm^{-1}. These frequencies are removed from the calculation of the vibrational partition function and are replaced by free translational or rotational contributions.

The reaction rate coefficients of elementary reaction steps are calculated on the basis of transition state theory:

$$k_{TST}(T) = \frac{k_B T Q_{TS}(T)}{h \quad Q_R(T)} \exp\left(-\frac{\Delta E^{\ddagger}}{RT}\right) \qquad \text{(S2)}$$

where k_B is Boltzmann constant, h is Planck constant and $\Delta E^{\ddagger}$ is the electronic activation barrier at 0 K (including the zero-point vibrational energy). Q_{TS} and Q_R denote the canonical partition functions of the transition and reactant state respectively. Arrhenius pre-exponential factors (A) and activation energies (E_a) are obtained by regression of Eq. S2 in the temperature range of 300 – 800 K.

(S2) Reaction network

As DFT-calculated reaction enthalpies and entropies can differ from NIST experimental values, it is necessary to correct these values from DFT to be chemically correct. Our correction approach is as follows; gas phase species in our network are corrected. In other words, every reaction step containing a gas phase component is corrected, so not only adsorption/desorption steps, but also Elay-Rideal type mechanisms or steps where reaction and desorption occur simultaneous. The DFT-based errors are divided over the product gas phase species, without altering any reagent gas phase energies (BuOH or EtOH), because this would mean that the whole energy diagram of the reaction network would shift. Below, a complete reaction network without modifications is shown. Followed by the same network to which NIST corrections are applied. Finally, we show the complete network with the kinetic parameters that are used for the simulations, i.e. with parameters varying within chemical accuracy and 1 parameter that is actually regressed against the experimental results.

We started our NIST corrections on the reaction of n-butanol to 1-butene:

$$\text{n-butanol}_{(g)} \rightarrow \text{1-butene}_{(g)} + H_2O_{(g)}$$

For which the energetics at 500 K are:

Table S1. NIST and DFT-based reaction energetics for the dehydration of n-butanol$_{(g)}$ to 1-butene$_{(g)}$ and $H_2O_{(g)}$

	ΔH_r (kJ mol^{-1})	ΔS_r (J mol^{-1} K^{-1})	ΔG_r (kJ mol^{-1})
NIST	36.47	139.17	-33.12

DFT	46.86	158.37	-32.33
Difference	-10.39	19.2	-0.79

Then we divide the error equally over the reaction products as shown in the following tables.

Table S2. NIST and DFT-based gas phase energetics of 1-butene

	H_g^0 (kJ mol^{-1})	S_g^0 (J mol^{-1} K^{-1})
DFT	-5991.92	354.80
NIST corrected DFT	-5997.11	345.20
Difference	-5.19	9.60

Table S3. NIST and DFT-based gas phase energetics of H_2O

	H_g^0 (kJ mol^{-1})	S_g^0 (J mol^{-1} K^{-1})
DFT	-1301.20	212.64
NIST corrected DFT	-1306.39	203.04
Difference	-5.19	9.60

Based on these corrections, all other gas phase reactions have a set correction for the other products, e.g. for the formation of dibutyl ether, 2 $BuOH_{(g)}$ molecules are needed and also $H_2O_{(g)}$ is formed, for which all gas phase thermodynamics are now set. But also for ethanol reactions this sets all further corrections. The summary of these corrections is found in the next few tables.

Table S4. NIST and DFT-based gas phase energetics of dibutyl ether

	H_g^0 (kJ mol^{-1})	S_g^0 (J mol^{-1} K^{-1})
DFT	-13401.69	592.84
NIST corrected DFT	-13390.62	596.52
Difference	11.07	3.68

Table S5. NIST and DFT-based gas phase energetics of trans-2-butene

	H_g^0 (kJ mol^{-1})	S_g^0 (J mol^{-1} K^{-1})
DFT	-6006.25	356.86
NIST corrected DFT	-6008.46	333.62
Difference	-2.21	-23.24

Table S6. NIST and DFT-based gas phase energetics of cis-2-butene

	H_g^0 (kJ mol^{-1})	S_g^0 (J mol^{-1} K^{-1})
DFT	-6002.52	358.68
NIST corrected DFT	-6005.51	336.19
Difference	-2.99	-22.49

Table S7. NIST and DFT-based gas phase energetics of ethyl butyl ether

	H_g^0 (kJ mol^{-1})	S_g^0 (J mol^{-1} K^{-1})
DFT	-10359.77	499.29
NIST corrected DFT	-10354.02	510.45
Difference	5.75	11.16

Table S8. NIST and DFT-based gas phase energetics of ethylene

NIST or DFT	H_g^0 (kJ mol^{-1})	S_g^0 (J mol^{-1} K^{-1})
DFT	-2937.33	246.60
NIST corrected DFT	-2946.97	246.50
Difference	-9.64	-0.10

Table S9. NIST and DFT-based gas phase energetics of diethyl ether

NIST or DFT	H_g^0 (kJ mol^{-1})	S_g^0 (J mol^{-1} K^{-1})
DFT	-7318.72	400.02
NIST corrected DFT	-7315.47	412.39
Difference	3.25	12.37

The full NIST-corrected DFT-based reaction network with reaction enthalpies, entropies, and kinetic parameters is listed in Table S10.

Table S10. All elementary reaction steps considered in the microkinetic model and DFT-based reaction energetics and kinetic parameters from [4-7]. Green text indicates NIST-corrections are applied on these gas-phase species.

	Elementary steps	${}^{a}\Delta H_r^0$	${}^{a}\Delta S_r^0$	$E_{a(f)}$	A_f	$k_{f(500K)}$
	n-butanol related reaction steps					
(R0)	$BuOH_{(g)}$ + * ⇌ $M1_B$	-146	-193	-	-	-
(R1)	$M1_B$ ⇌ W + 1-$butene_{(g)}$	102	190	177	1.2×10^{15}	4.0×10^{-4}
(R2)	W ⇌ $H_2O(g)$	80	142	-	-	-
(R3)	$M1_B$ ⇌ $C1_B$	75	79	140	3.1×10^{14}	7.3×10^{-1}
(R4)	$C1_B$ ⇌ W + 1-$butene_{(g)}$	27	111	-	-	-
(R5)	$M1_B$ ⇌ $M2_B$	82	-5	-	-	-
(R6)	$M2_B$ ⇌ 1-butene* + $H_2O_{(g)}$	23	191	46	9.7×10^{14}	1.6×10^{10}
(R7)	1-butene* ⇌ 1-$butene_{(g)}$ + *	77	146	-	-	-
(R8)	$M2_B$ ⇌ Butoxy + $H_2O_{(g)}$	17	156	50	3.7×10^{14}	2.2×10^{9}
(R9)	butoxy ⇌ 1-butene*	6	35	94	3.8×10^{13}	6.1×10^{3}
(R10)	$M1_B$ + $BuOH_{(g)}$ ⇌ $D1_{BB}$	-125	-183	-	-	-
(R11)	$D1_{BB}$ ⇌ $D2_{BB}$	43	-3	-	-	-
(R12)	$D2_{BB}$ ⇌ $C2_B$ + 1-$butene_{(g)}$	63	156	119	3.1×10^{14}	1.1×10^{2}
(R13)	$C2_B$ ⇌ $M1_B$ + $H_2O_{(g)}$	56	170	-	-	-
(R14)	$D2_{BB}$ ⇌ DBE* + $H_2O_{(g)}$	10	148	102	1.5×10^{14}	3.6×10^{3}
(R15)	DBE* ⇌ $DBE_{(g)}$ + *	201	213	-	-	-
(R16)	Butoxy + $BuOH_{(g)}$ ⇌ $C3_{BB}$	-94	-173	-	-	-
(R17)	$C3_{BB}$ ⇌ DBE* (S_N2)	-77	-16	61	3.1×10^{12}	1.3×10^{6}
(R18)	$C3_{BB}$ ⇌ DBE* (S_N1)	-77	-16	111	7.7×10^{13}	1.7×10^{2}
(R19)	DBE* ⇌ $C4_{BB}$	103	52	166	2.7×10^{14}	1.3×10^{-3}
(R20)	$C4_{BB}$ ⇌ 1-butene* + $BuOH_{(g)}$	75	173	-	-	-
(R21)	DBE* ⇌ DBE2	63	9	-	-	-
(R22)	DBE2 ⇌ 1-butene* + $BuOH_{(g)}$	115	215	85	1.7×10^{13}	2.3×10^{4}
(R23)	$D1_{BB}$ ⇌ $C2_B$ + trans-2-$butene_{(g)}$	95	141	165	4.9×10^{15}	2.8×10^{-2}
(R24)	DBE* ⇌ $M1_B$ + trans-2-$butene_{(g)}$	97	166	174	4.1×10^{15}	4.9×10^{-3}
(R25)	1-Butene* ⇌ trans-2-butene*	-23	1	51	1.8×10^{12}	8.6×10^{6}
(R26)	Trans-2-butene* ⇌ trans-2-$butene_{(g)}$ + *	88	134	-	-	-
(R27)	1-butene* ⇌ 2-Butoxy	-24	-80	48	2.7×10^{9}	2.6×10^{4}
(R28)	2-Butoxy ⇌ trans-2-butene*	2	80	68	1.0×10^{14}	7.9×10^{6}
(R29)	2-Butoxy ⇌ cis-2-butene*	17	71	74	5.5×10^{13}	1.0×10^{6}

(R30)	cis-2-butene* ⇌ cis-2-butene$_{(g)}$ + *	76	145	-	-	-
(R31)	$D1_{BB}$ ⇌ $C2_B$ + cis-2-butene$_{(g)}$	98	143	165	4.9×10^{15}	2.8×10^{-2}
(R32)	DBE* ⇌ $M1_B$ + cis-2-butene$_{(g)}$	100	169	171	3.8×10^{15}	5.2×10^{-3}
	Ethanol related reaction steps					
(R33)	$EtOH_{(g)}$ + * ⇌ $M1_E$	-124	-168	-	-	-
(R34)	$M1_E$ ⇌ $M2_E$	14	7	-	-	-
(R35)	$M2_E$ ⇌ Ethoxy + $H_2O_{(g)}$	71	137	119	4.3×10^{13}	1.6×10^{1}
(R36)	Ethoxy -> Ethene*	44	60	107	9.6×10^{12}	6.9×10^{1}
(R37)	Ethene* ⇌ $C_2H_{4(g)}$ + *	41	99	-	-	-
(R38)	$M1_E$ + $EtOH_{(g)}$ ⇌ $D1_{EE}$	-99	-162	-	-	-
(R39)	$D1_{EE}$ ⇌ $D2_{EE}$	44	24	-	-	-
(R40)	$D2_{EE}$ ⇌ DEE* + $H_2O_{(g)}$	11	116	92	1.2×10^{13}	2.7×10^{3}
(R41)	DEE* ⇌ $DEE_{(g)}$ + tfree	144	178	-	-	-
(R42)	DEE* ⇌ $C1_{EE}$	114	51	145	4.8×10^{13}	3.1×10^{-2}
(R43)	$C1_{EE}$ ⇌ Ethene* + $EtOH_{(g)}$	58	175	-	-	-
(R44)	Ethoxy + $EtOH_{(g)}$ ⇌ DEE*	-129	-166	18	4.3×10^{4}	5.5×10^{2}
(R45)	$D2_{EE}$ ⇌ $C2_E$ + $C_2H_{4(g)}$	47	131	111	4.0×10^{12}	1.1×10^{1}
(R46)	$C2_E$ -⇌ $M1_E$ + $H_2O_{(g)}$	54	143	-	-	-
(R47)	$M1_E$ ⇌ W + $C_2H_{4(g)}$	90	162	181	5.7×10^{14}	6.7×10^{-5}
(R48)	$M2_E$ ⇌ $C3_E$	84	63	129	2.0×10^{13}	6.1×10^{-1}
(R49)	$C3_E$ ⇌ W+ $C_2H_{4(g)}$	-9	91	-	-	-
(R50)	W +$EtOH_{(g)}$ ⇌ $C2_E$	-97	-169	-	-	-
(R51)	$C2_E$ ⇌ 2W + $C_2H_{4(g)}$	68	151	176	1.4×10^{15}	5.8×10^{-4}
(R52)	2W ⇌ W + $H_2O_{(g)}$	76	153	-	-	-
	Mixed alcohol reaction steps					
(R53)	$M1_B$ + $EtOH_{(g)}$ ⇌ $D1_{BE}$	-98	-151	-	-	-
(R54)	$D1_{BE}$ ⇌ $D2_{BE}$	43	20	-	-	-
(R55)	$D2_{BE}$ ⇌ BEE* + $H_2O_{(g)}$	6	113	91	2.1×10^{12}	6.1×10^{2}
(R56)	BEE* ⇌ $EBE_{(g)}$ + *	173	201	-	-	-
(R57)	$M1_E$ + $BuOH_{(g)}$ ⇌ $D1_{EB}$	-128	-179	-	-	-
(R58)	$D1_{EB}$ ⇌ $D2_{EB}$	46	19	-	-	-
(R59)	$D2_{EB}$ ⇌ EBE* + $H_2O_{(g)}$	11	116	90	2.1×10^{12}	9.2×10^{2}
(R60)	EBE* ⇌ $EBE_{(g)}$	174	203	-	-	-
(R61)	Butoxy + $EtOH_{(g)}$ ⇌ $C3_{BE}$	-41	-129	-	-	-

(R62)	$C3_{BE}$ ⇌ BEE*	-106	-39	30	3.8×10^{11}	3.0×10^{8}
(R63)	Ethoxy + $BuOH_{(g)}$ ⇌ $C3_{EB}$	-71	-165	-	-	-
(R64)	$C3_{EB}$ ⇌ EBE*	-85	-24	42	9.4×10^{11}	3.8×10^{7}
(R65)	BEE* ⇌ $C4_{BE}$	97	59	141	2.8×10^{14}	2.2×10^{-1}
(R66)	$C4_{BE}$ ⇌ 1-butene* + $EtOH_{(g)}$	57	145	-	-	-
(R67)	EBE* ⇌ $C4_{EB}$	114	62	143	5.3×10^{13}	5.9×10^{-2}
(R68)	$C4_{EB}$ ⇌Ethene* + $BuOH_{(g)}$	86	187	-	-	-
(R69)	BEE* ⇌ BEE2	60	11	-	-	-
(R70)	BEE2 ⇌ 1-butene* + $EtOH_{(g)}$	93	193	85	9.7×10^{12}	1.2×10^{4}
(R71)	EBE* ⇌ EBE2	60	0	-	-	-
(R72)	EBE2 ⇌ Ethene* + $BuOH_{(g)}$	140	249	96	1.5×10^{13}	1.5×10^{3}
(R73)	$D2_{BE}$ ⇌ $C2_{E}$ + 1-$butene_{(g)}$	59	152	124	6.1×10^{12}	7.0×10^{-1}
(R74)	$D2_{EB}$ ⇌ $C2_{B}$ + $C_2H_{4(g)}$	50	102	116	5.5×10^{12}	4.5×10^{0}

Next to these NIST-corrections, we allowed all states in the network to vary within chemical accuracy, i.e. adsorbed species, energy barriers were allowed to vary within 4 kJ mol^{-1}. The complete reaction mechanism with modified kinetic parameters (within chemical accuracy, indicated in blue) and regressed parameter (indicated in red) are shown in Table S11.

Table S11. All elementary reaction steps considered in the microkinetic model and DFT-based reaction energetics and kinetic parameters from [4-7]. Green text indicates NIST-corrections are applied on these gas-phase species. Blue text indicates altered within chemical accuracy and orange text indicates regressed parameter.

	Elementary steps	${}^{a}\Delta H_r^0$	${}^{a}\Delta S_r^0$	$E_{a(f)}$	A_f	$k_{f(500K)}$
	n-butanol related reaction steps					
(R0)	$BuOH_{(g)}$ + * ⇌ $M1_B$	-146	-193	-	-	-
(R1)	$M1_B$ ⇌ W + 1-$butene_{(g)}$	102	190	177	1.2×10^{15}	4.0×10^{-4}
(R2)	W ⇌ $H_2O(g)$	80	142	-	-	-
(R3)	M1 ⇌ C1	75	79	140	3.1×10^{14}	7.3×10^{-1}
(R4)	C1 ⇌ W + 1-$butene_{(g)}$	27	111	-	-	-
(R5)	$M1_B$ ⇌ $M2_B$	82	-5	-	-	-
(R6)	$M2_B$ ⇌ 1-butene* + $H_2O_{(g)}$	19	191	46	9.7×10^{14}	1.6×10^{10}
(R7)	1-butene* ⇌ 1-$butene_{(g)}$ + *	81	146	-	-	-
(R8)	$M2_B$ ⇌ Butoxy + $H_2O_{(g)}$	17	156	50	3.7×10^{14}	2.2×10^{9}
(R9)	butoxy ⇌ 1-butene*	2	35	94	3.8×10^{13}	6.1×10^{3}
(R10)	$M1_B$ + $BuOH_{(g)}$ ⇌ $D1_{BB}$	-125	-183	-	-	-
(R11)	$D1_{BB}$ ⇌ $D2_{BB}$	43	-3	-	-	-
(R12)	$D2_{BB}$ ⇌ $C2_B$ + 1-$butene_{(g)}$	63	156	119	3.1×10^{14}	1.1×10^{2}
(R13)	$C2_B$ ⇌ $M1_B$ + $H_2O_{(g)}$	56	170	-	-	-
(R14)	$D2_{BB}$ ⇌ DBE* + $H_2O_{(g)}$	13	148	102	1.5×10^{14}	3.6×10^{3}
(R15)	DBE* ⇌ $DBE_{(g)}$ + *	198	213	-	-	-
(R16)	Butoxy + $BuOH_{(g)}$ ⇌ $C3_{BB}$	-94	-173	-	-	-
(R17)	$C3_{BB}$ ⇌ DBE* (S_N2)	-74	-16	61	3.1×10^{12}	1.3×10^{6}
(R18)	$C3_{BB}$ ⇌ DBE* (S_N1)	-74	-16	111	7.7×10^{13}	1.7×10^{2}
(R19)	DBE* ⇌ $C4_{BB}$	100	52	166	2.7×10^{14}	1.3×10^{-3}
(R20)	$C4_{BB}$ ⇌ 1-butene* + $BuOH_{(g)}$	71	173	-	-	-
(R21)	DBE* ⇌ DBE2	63	9	-	-	-
(R22)	DBE2 ⇌ 1-butene* + $BuOH_{(g)}$	115	215	85	1.7×10^{13}	2.3×10^{4}
(R23)	$D1_{BB}$ ⇌ $C2_B$ + trans-2-$butene_{(g)}$	95	141	165	4.9×10^{15}	2.8×10^{-2}
(R24)	DBE* ⇌ $M1_B$ + trans-2-$butene_{(g)}$	94	166	177	4.1×10^{15}	4.9×10^{-3}
(R25)	1-butene* ⇌ trans-2-butene*	-19	1	51	6.8×10^{11}	3.3×10^{6}
(R26)	Trans-2-butene* ⇌ trans-2-$butene_{(g)}$ + *	88	134	-	-	-
(R27)	1-butene* ⇌ 2-Butoxy	-24	-80	44	2.7×10^{9}	6.9×10^{4}
(R28)	2-Butoxy ⇌ trans-2-butene*	2	80	68	1.0×10^{14}	7.9×10^{6}
(R29)	2-Butoxy ⇌ cis-2-butene*	21	71	70	5.5×10^{13}	2.7×10^{6}

(R30)	cis-2-butene* ⇌ cis-2-butene$_{(g)}$ + *	76	145	-	-	-
(R31)	$D1_{BB}$ ⇌ $C2_B$ + cis-2-butene$_{(g)}$	98	143	164	4.9×10^{15}	3.8×10^{-2}
(R32)	DBE* ⇌ $M1_B$ + cis-2-butene$_{(g)}$	100	169	172	3.8×10^{15}	4.2×10^{-3}
	Ethanol related reaction steps					
(R33)	$EtOH_{(g)}$ + * ⇌ $M1_E$	-124	-168	-	-	-
(R34)	$M1_E$ ⇌ $M2_E$	14	7	-	-	-
(R35)	$M2_E$ ⇌ Ethoxy + $H_2O_{(g)}$	71	137	119	4.3×10^{13}	1.6×10^{1}
(R36)	Ethoxy -> Ethene*	44	60	107	9.6×10^{12}	6.9×10^{1}
(R37)	Ethene* ⇌ $C_2H_{4(g)}$ + *	41	99	-	-	-
(R38)	$M1_E$ + $EtOH_{(g)}$ ⇌ $D1_{EE}$	-102	-162	-	-	-
(R39)	$D1_{EE}$ ⇌ $D2_{EE}$	44	24	-	-	-
(R40)	$D2_{EE}$ ⇌ DEE* + $H_2O_{(g)}$	11	116	89	1.2×10^{13}	6.4×10^{3}
(R41)	DEE* ⇌ $DEE_{(g)}$ + tfree	144	178	-	-	-
(R42)	DEE* ⇌ $C1_{EE}$	114	51	145	4.8×10^{13}	3.1×10^{-2}
(R43)	$C1_{EE}$ ⇌ Ethene* + $EtOH_{(g)}$	58	175	-	-	-
(R44)	Ethoxy + $EtOH_{(g)}$ ⇌ DEE*	-129	-166	18	4.3×10^{4}	5.5×10^{2}
(R45)	$D2_{EE}$ ⇌ $C2_E$ + $C_2H_{4(g)}$	50	131	111	4.0×10^{12}	1.1×10^{1}
(R46)	$C2_E$ -⇌ $M1_E$ + $H_2O_{(g)}$	54	143	-	-	-
(R47)	$M1_E$ ⇌ W + $C_2H_{4(g)}$	90	162	181	5.7×10^{14}	6.7×10^{-5}
(R48)	$M2_E$ ⇌ $C3_E$	84	63	129	2.0×10^{13}	6.1×10^{-1}
(R49)	$C3_E$ ⇌ W+ $C_2H_{4(g)}$	-9	91	-	-	-
(R50)	W +$EtOH_{(g)}$ ⇌ $C2_E$	-97	-169	-	-	-
(R51)	$C2_E$ ⇌ 2W + $C_2H_{4(g)}$	68	151	176	1.4×10^{15}	5.8×10^{-4}
(R52)	2W ⇌ W + $H_2O_{(g)}$	76	153	-	-	-
	Mixed alcohol reaction steps					
(R53)	$M1_B$ + $EtOH_{(g)}$ ⇌ $D1_{BE}$	-99	-151	-	-	-
(R54)	$D1_{BE}$ ⇌ $D2_{BE}$	43	20	-	-	-
(R55)	$D2_{BE}$ ⇌ BEE* + $H_2O_{(g)}$	8	113	93	2.1×10^{12}	3.8×10^{2}
(R56)	BEE* ⇌ $EBE_{(g)}$ + *	173	201	-	-	-
(R57)	$M1_E$ + $BuOH_{(g)}$ ⇌ $D1_{EB}$	-129	-179	-	-	-
(R58)	$D1_{EB}$ ⇌ $D2_{EB}$	46	19	-	-	-
(R59)	$D2_{EB}$ ⇌ EBE* + $H_2O_{(g)}$	12	116	92	2.1×10^{12}	5.7×10^{2}
(R60)	EBE* ⇌ $EBE_{(g)}$	174	203	-	-	-
(R61)	Butoxy + $EtOH_{(g)}$ ⇌ $C3_{BE}$	-41	-129	-	-	-

(R62)	$C3_{BE}$ ⇌ BEE*	-106	-39	32	3.8×10^{11}	1.9×10^{8}
(R63)	Ethoxy + $BuOH_{(g)}$ ⇌ $C3_{EB}$	-71	-165	-	-	-
(R64)	$C3_{EB}$ ⇌ EBE*	-85	-24	42	9.4×10^{11}	3.8×10^{7}
(R65)	BEE* ⇌ $C4_{BE}$	97	59	141	2.8×10^{14}	2.2×10^{-1}
(R66)	$C4_{BE}$ ⇌ 1-butene* + $EtOH_{(g)}$	53	145	-	-	-
(R67)	EBE* ⇌ $C4_{EB}$	114	62	143	5.3×10^{13}	5.9×10^{-2}
(R68)	$C4_{EB}$ ⇌Ethene* + $BuOH_{(g)}$	86	187	-	-	-
(R69)	BEE* ⇌ BEE2	60	11	-	-	-
(R70)	BEE2 ⇌ 1-butene* + $EtOH_{(g)}$	89	193	85	9.7×10^{12}	1.2×10^{4}
(R71)	EBE* ⇌ EBE2	60	0	-	-	-
(R72)	EBE2 ⇌ Ethene* + $BuOH_{(g)}$	140	249	96	1.5×10^{13}	1.5×10^{3}
(R73)	$D2_{BE}$ ⇌ $C2_{E}$ + 1-butene$_{(g)}$	61	152	124	6.1×10^{12}	7.0×10^{-1}
(R74)	$D2_{EB}$ ⇌ $C2_{B}$ + $C_2H_{4(g)}$	51	102	99	5.5×10^{12}	2.4×10^{2}

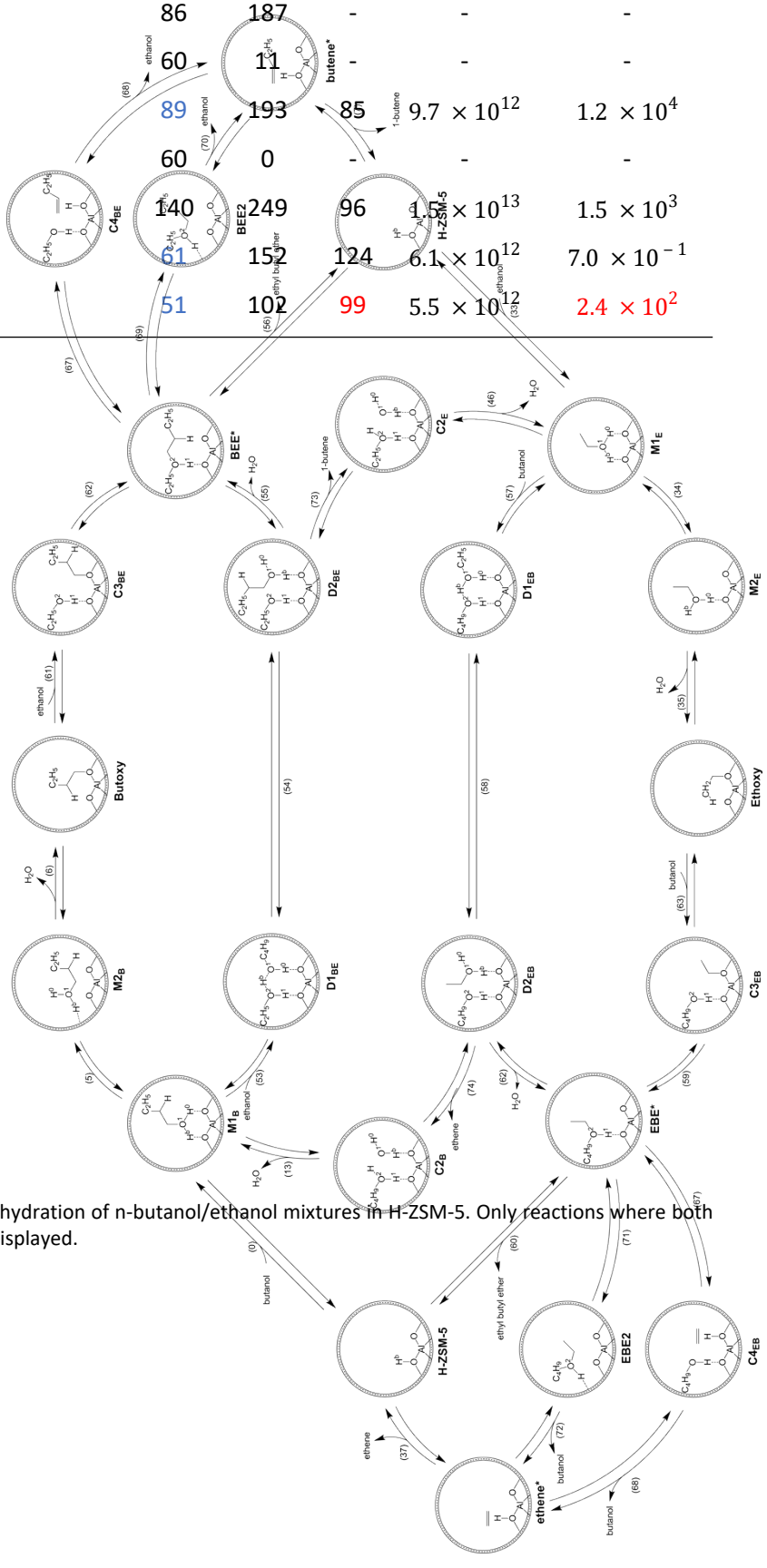

Figure S1. Detailed reaction network for dehydration of n-butanol/ethanol mixtures in H-ZSM-5. Only reactions where both alcohols or derivatives of are involved are displayed.

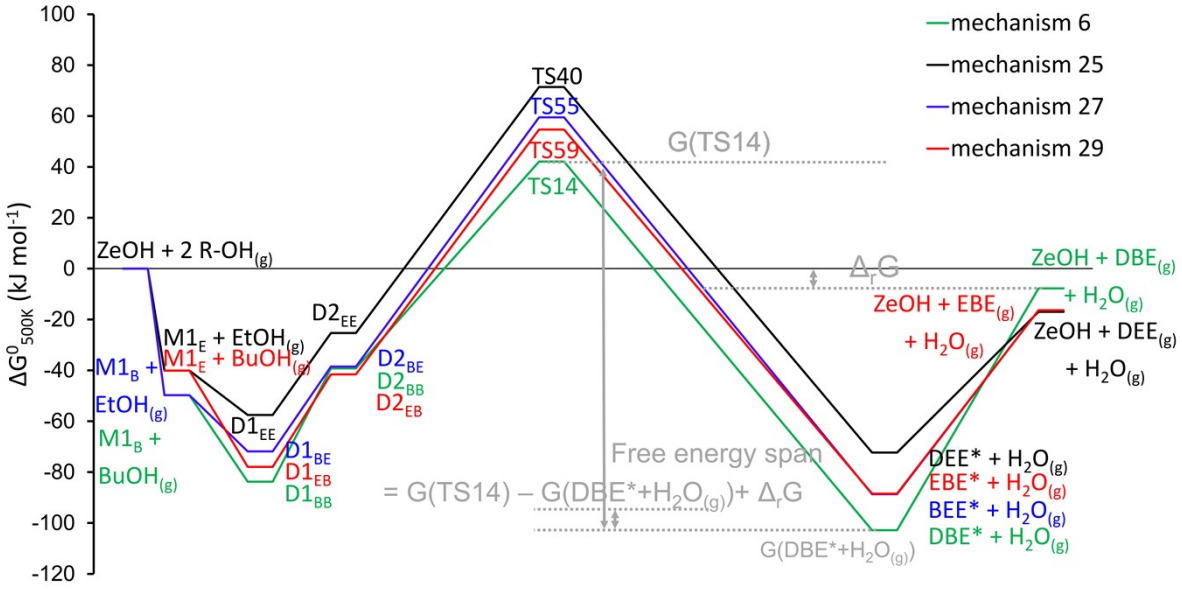

Figure S2. Illustration of the energetic span concept, applied to mechanism 6 of Figure 4.

(S3) Transition state analysis

(S3.1) EBE formation transition states

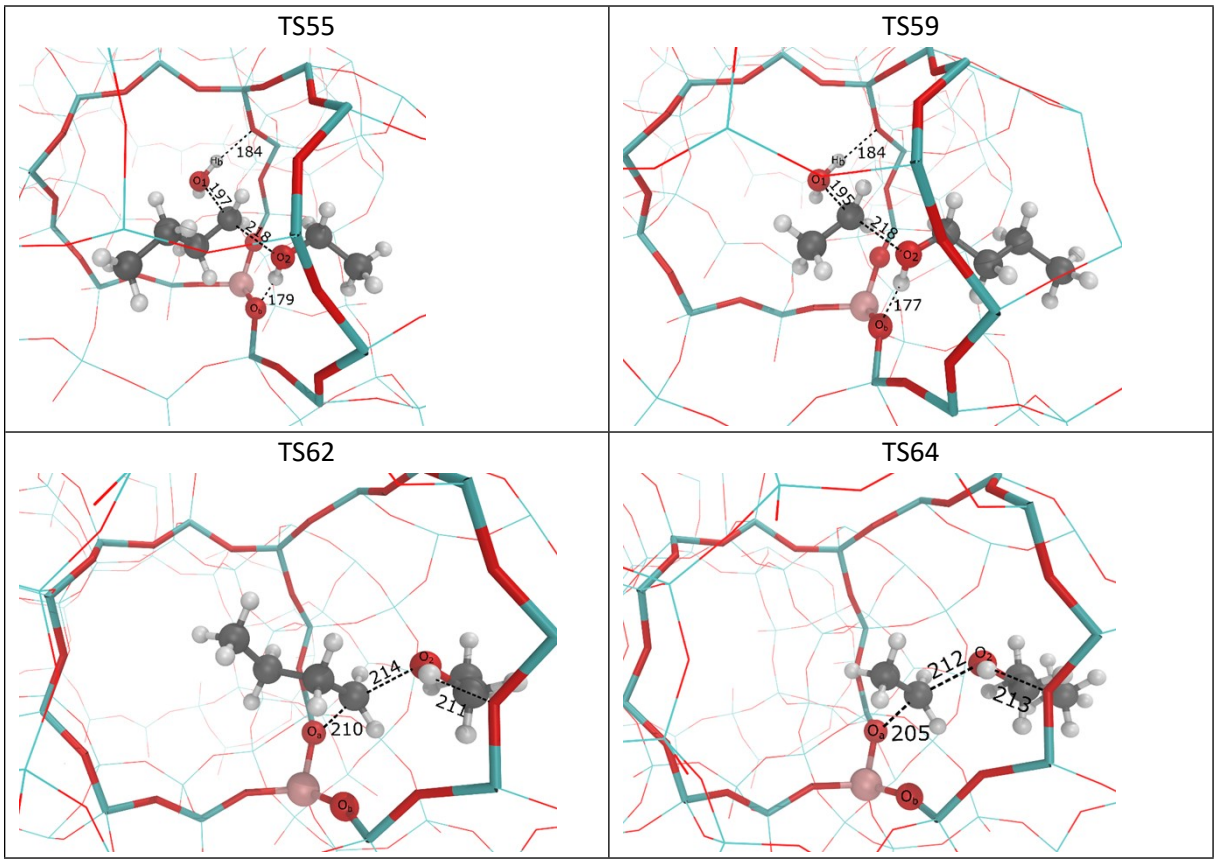

Figure S3. Transition state structures for ethyl butyl ether formation in H-ZSM-5. (1) TS55, mechanism 27, an SN2 substitution reaction of $D2_{BE}$ to ethyl butyl ether. (2) TS59, mechanism 29, an SN2 substitution reaction of $D2_{EB}$ to ethyl butyl ether. (3) TS62, mechanism 28, SN2 substitution of 1-butoxide and ethanol to ethyl butyl ether. (4) TS64, mechanism 30, SN2 substitution of ethoxide and butanol to ethyl butyl ether. Color code: silicon – cyan, oxygen – red, aluminum – pink, hydrogen – white, carbon – gray, hydrogen bonds, bonds breaking/forming – dashed lines.

Reaction mechanism 27 (butanol-ethanol dimer to ethyl butyl ether via SN2-type reaction)

In the activated step of the mechanism (step 55), the carbon bonded to O_1 of the protonated butanol breaks its bond with O_1 (allowing water to leave), and simultaneously forms a bond with O_2 of the physisorbed ethanol (see TS55 in Figure S3. The simultaneous formation of a new bond eases the breaking of the existing bond. For SN2-type reactions, the nucleophile (here O_2) and leaving group (here $-OH_2$), should be aligned directly opposing, with an angle close to 180° as in a trigonal bipyramidal structure. The angle between O_1-C-O_2 is 163.6°, largely due to the leaving water being stabilized by hydrogen bonding with a zeolite oxygen. The distance between O_1-C is 197 pm and O_2-C is 218 pm, thus the carbon atom is close to equidistant from both O_1 and O_2, indicating an SN2-type mechanism.

Reaction mechanism 28 (ethanol-butanol dimer to ethyl butyl ether via SN2-type reaction)

For the activated step, 59, the carbon of the protonated ethanol, bonded to O_1 is concurrently breaking the O_1-C bond and forming the C-O_2 bond with the physisorbed butanol. Geometrical analysis of TS59 shows that the angle between O_1-C-O_2 is 163.3°, again with similar bond lengths between O_1-C and C-O_2, indicating the SN2-type mechanism.

Reaction mechanism 29 (butoxide-mediated formation of ethyl butyl ether via SN2-type reaction)

For mechanism 29, step 62 is activated, inspection of TS62 shows that the distance between O_a and the butoxide carbon is 210 pm, and the distance of the carbon with O_2 of the physisorbed ethanol is 214 pm, i.e. the carbon is equidistant from both oxygens. Furthermore, the angle of O_a-C-O_2 is 159.2°. The geometry of TS62 is in line with the stereochemical requirements for an SN2-type mechanism.

Reaction mechanism 30 (ethoxide-mediated formation of ethyl butyl ether via SN2-type reaction)

For mechanism 30, step 64 is activated, where the bond between the zeolite oxygen (O_a) and carbon of the surface ethoxide is broken and simultaneously a bond is forming between the carbon and O_2 of the physisorbed n-butanol. Detailed analysis of TS64 shows that also here the carbon is at the center between these two oxygens, under an angle (O_a-C-O_2) of 164.5°, indicating an SN2-type mechanism.

(S3.2) EBE decomposition transition states

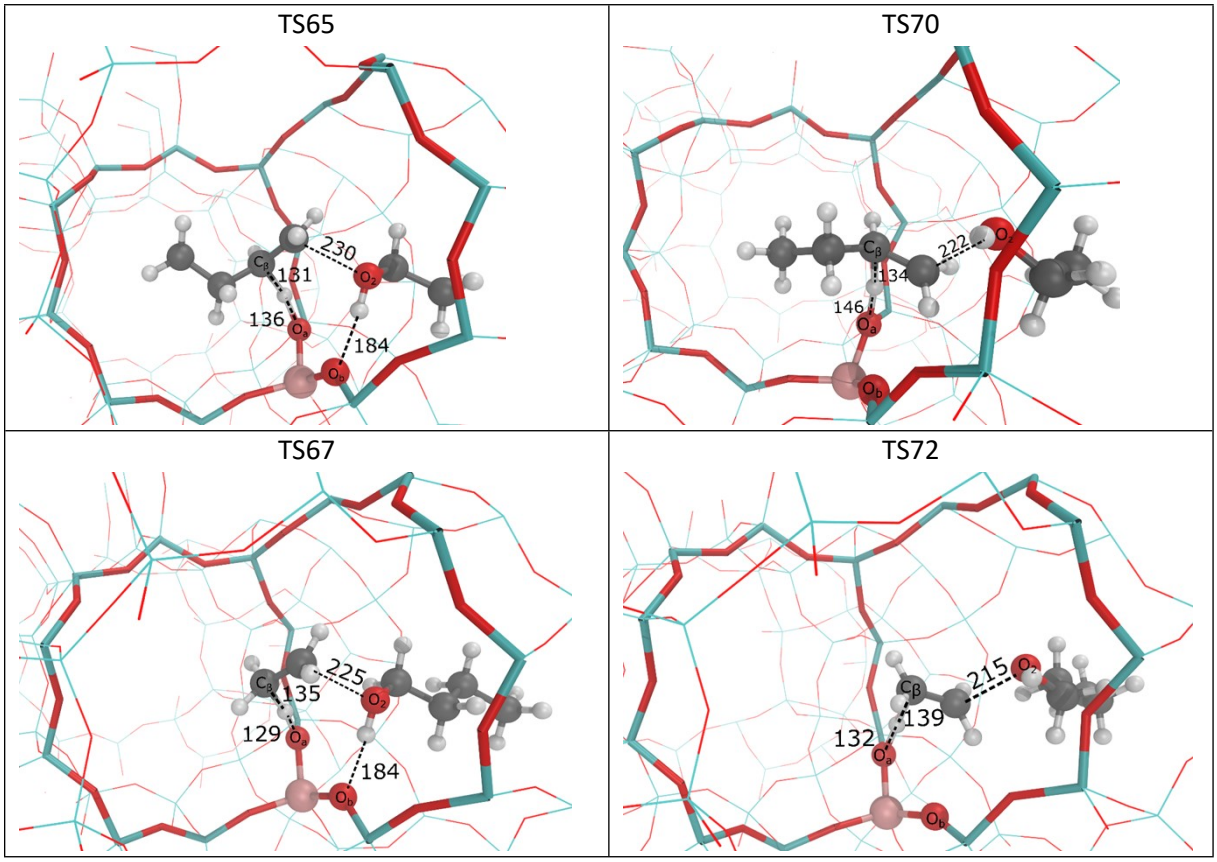

Figure S4. Ethyl butyl ether decomposition transition states in H-ZSM-5, view at the channel intersection: (1) TS65, mechanism 31, syn-elimination forming 1-butene and ethanol, (2) TS70, mechanism 32, anti-elimination forming 1-butene and ethanol, (3) TS67, mechanism 33, a syn-elimination leading to ethene and n-butanol, (4) TS72, mechanism 34, an anti-elimination leading to ethene and n-butanol. Colour code: silicon – cyan, oxygen – red, aluminum – pink, hydrogen – white, carbon – grey, hydrogen bonds, bonds breaking/forming – dashed lines.

Reaction Mechanism 31 (concerted ethyl butyl ether decomposition to 1-butene and ethanol)

Step 65 is activated, here the β-hydrogen and the ethanol leaving group have a near syn-coplanar structure, with an O_2-C_α-C_β-H_β dihedral angle of -13.6°. The C-O_2 bond of TS65 is broken to a larger extent than the C_β-H_β bond, indicating an elimination with E_1 characteristics. The interatomic distances of C-O_2 is 230 pm, of C_β-H_β is 131 pm and of O_a-H_β is 136 pm, indicating that the C-O_2 and C_β-H_β bonds are nearly broken.

Reaction mechanism 32 (E2 elimination of ethyl butyl ether to 1-butene and ethanol)

Step 70 is activated and similar to step 65, but instead of being syn-coplanar, here the transition state has an anti-periplanar configuration. This is reflected in the dihedral angle of -178.7° for O_2-C_α-C_β-H_β. The bond lengths of O_2-C is 222 pm, of C_β-H_β is 134 pm, of C_α-C_β is 138 pm and of O_a-H_β is 146 pm.

Reaction mechanism 33 (concerted syn elimination of ethyl butyl ether to ethene and n-butanol)

Step 67 is activated, here the β-hydrogen and n-butanol leaving group have a syn-coplanar structure, with an O_2-C_α-C_β-H_β dihedral angle of -10.4°. The C-O_2 bond length is elongated to 225 pm, the C_β-H_β bond length to 135 pm, the O_a- H_β bond length is 129 pm.

Reaction mechanism 34 (E2 elimination of ethyl butyl ether to ethene and n-butanol)
Here step 72 is activated and similar to step 70. The O_2-C_α-C_β-H_β dihedral angle is -175.4°, indicating the anti-elimination configuration. Similar as for TS67 compared to TS65, also here the C-O_2 bond is broken to a lesser extent compared to TS70, whilst the C_β-H_β bond breakage is more pronounced. All ethyl butyl ether decomposition mechanisms have late transition states, close to their respective products.

(S3.3) Alcohol assisted dehydration transition states

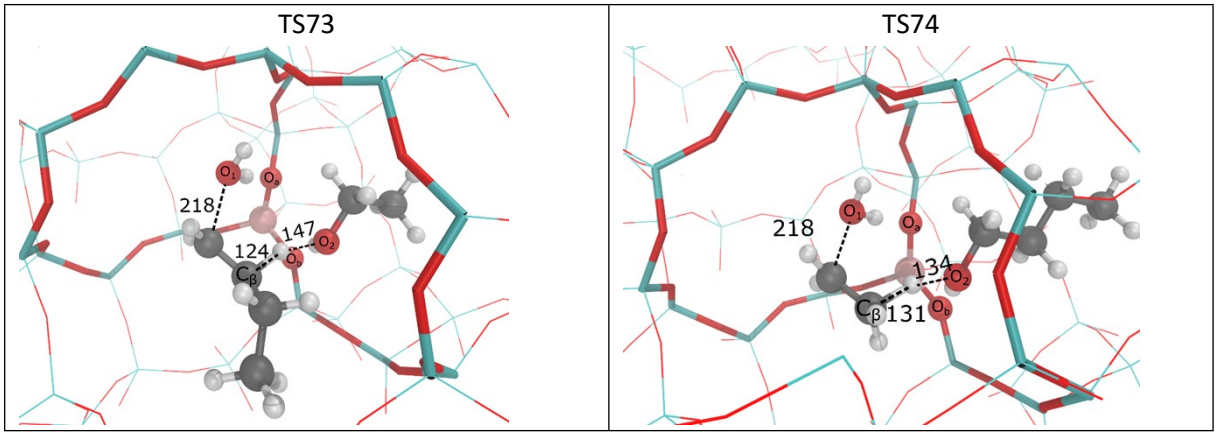

Figure S5. Alcohol-assisted dehydration transition states in H-ZSM-5, view at the channel intersection: (1) TS73, mechanism 35, 1,2-syn-elimination forming 1-butene, (2) TS74, mechanism 36, 1,2-syn-elimination forming ethane. Colour code: silicon – cyan, oxygen – red, aluminum – pink, hydrogen – white, carbon – grey, hydrogen bonds, bonds breaking/forming – dashed lines.

(S4) Experimental details

The experiments are performed, following an identical procedure as by de Reviere et al. [8].

Kinetic experiments for n-butanol/ethanol dehydration over H-ZSM-5 are utilized to validate our theoretical model results. A commercial powder zeolite NH_4-MFI with Si/Al of 15 (Zeolyst, CBV 3024E) was employed for the catalytic testing. The zeolite powder in NH_4-form is calcined under an air flow at 823 K for 4 hours to convert it into its protonated form, referred as H-ZSM-5. Catalyst particles within 100 – 150 μm range are prepared by pelletizing and sequential sieving of the H-ZSM-5 zeolite. Based on NH_3-TPD measurements, the strong acid site concentration, which has been linked to catalytic activity, is measured to be 0.257 mol kg^{-1}. In the study of Alexopoulos et al. it was shown that experiments obtained with this material could be compared with the theoretical results for ethanol dehydration [7].

The catalytic tests in this work are performed in a tubular reactor with a length of 0.85 m and internal diameter of 2.2 mm [9]. The catalyst is diluted with inert α-Al_2O_3 in a 10/1 ratio of inert/catalyst, to

avoid hot and cold spots. Mixtures of liquid n-butanol (Merck, > 99.5%) and ethanol (ChemLab, > 99.8%, absolute) in a 6/1 mass ratio (as obtained from ABE fermentation) are sent through a Coriolis mass flow controller. Nitrogen is used as a carrier gas, of which the flow rate can be varied to adjust the partial pressure of the alcohol mixture without altering the site time.

The experimental data obtained at 513 K is as reported in [8], the experimental data obtained at 503 K is new for this work, to have a larger dataset at butanol conversion below 100% in a broad site time coverage. At higher temperatures, full conversion is reached at too low site times to have an extensive data set that can be modeled. Beyond full conversion, secondary reactions such as oligomerization and cracking occur, which are not embedded in the present microkinetic model, which is designed to describe alcohol dehydration. Therefore the microkinetic model cannot be used in that regime and additional experimental data at a lower temperature is presented in this work. Table S12 lists all new experimental data. Experimental flow rates are 6 g hr^{-1}.

Table S12. Experimental dataset obtained at 503 K as reported in this work. S_{EBE} has two values, as it is calculated both from a BuOH point of view and an EtOH point of view.

Site time	X_{BuOH} | X_{EtOH}	$S_{1\text{-butene}}$	$S_{trans\text{-}2\text{-}butene}$	$S_{cis\text{-}2\text{-}butene}$	S_{DBE}	S_{EBE} (BuOH |EtOH)	S_{Ethene}	S_{DEE}
1.34	0.36 | 0.15	0.17	0.21	0.16	0.38	0.07 | 0.67	0.21	0.12
1.59	0.40 | 0.15	0.17	0.23	0.17	0.35	0.07 | 0.72	0.17	0.10
1.89	0.43 | 0.17	0.17	0.24	0.18	0.33	0.07 | 0.66	0.21	0.12
2.21	0.44 |0.16	0.17	0.26	0.19	0.31	0.07 | 0.68	0.19	0.14
3.71	0.66 | 0.27	0.17	0.33	0.24	0.18	0.07 | 0.66	0.17	0.17
4.39	0.70 | 0.25	0.17	0.36	0.26	0.14	0.07 | 0.69	0.14	0.17

(S5) Microkinetic simulation without fitted parameter

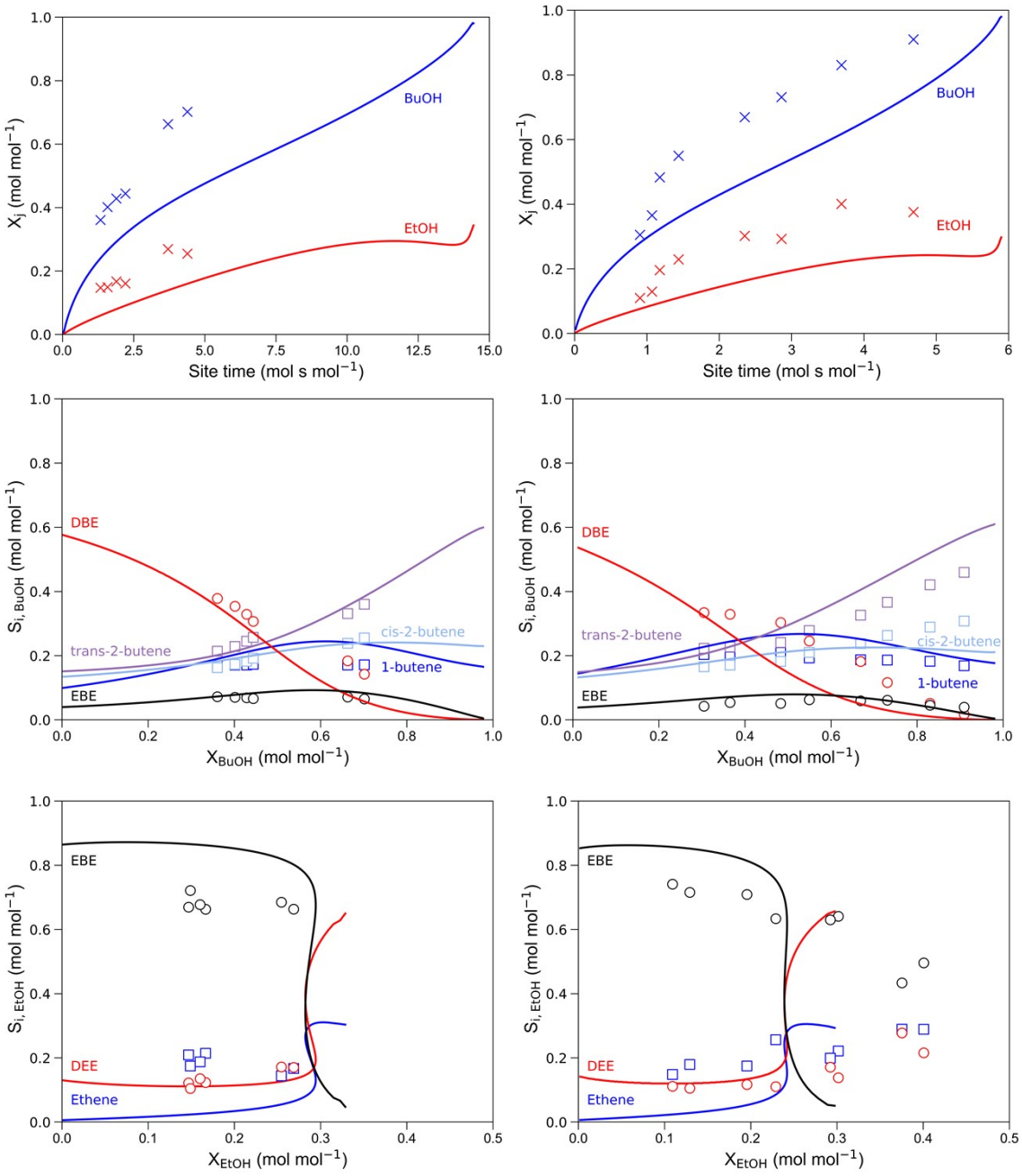

Figure S6. Experimental and simulated conversion of n-butanol (ᔕ) and ethanol (ᔕ) versus site time (top), catalyzed by H-ZSM-5, selectivity of products from n-butanol versus butanol conversion X_{BuOH} (middle) and selectivity of products of ethanol versus X_{EtOH} (bottom). Temperature = 503 K (left) and 513 K right), total pressure = 5 Bar, p^0_{BuOH} = 29 kPa, p^0_{EtOH} = 7.8 kPa. Full lines are simulation results.

(S6) TOFs of mechanisms 6 to 26

As an illustration, the TOFs of mechanisms 6 to 26 are listed here as a function of conversion. These mechanisms are part of the “pure n-butanol dehydration” and “pure ethanol dehydration” and have been extensively studied by John et al., Gunst et al. and Alexopoulos et al., our results are for obvious

reasons very similar to their results: the reaction parameters of their simulations are either unaltered or altered with maximally 4 kJ mol^{-1}. Hence, no fundamental differences in trends are observed within a reaction pathway. Nevertheless, there are some unavoidable differences, as the reaction network studied here encompasses more reactions, surface species,.. thus active site coverage effects can be present.

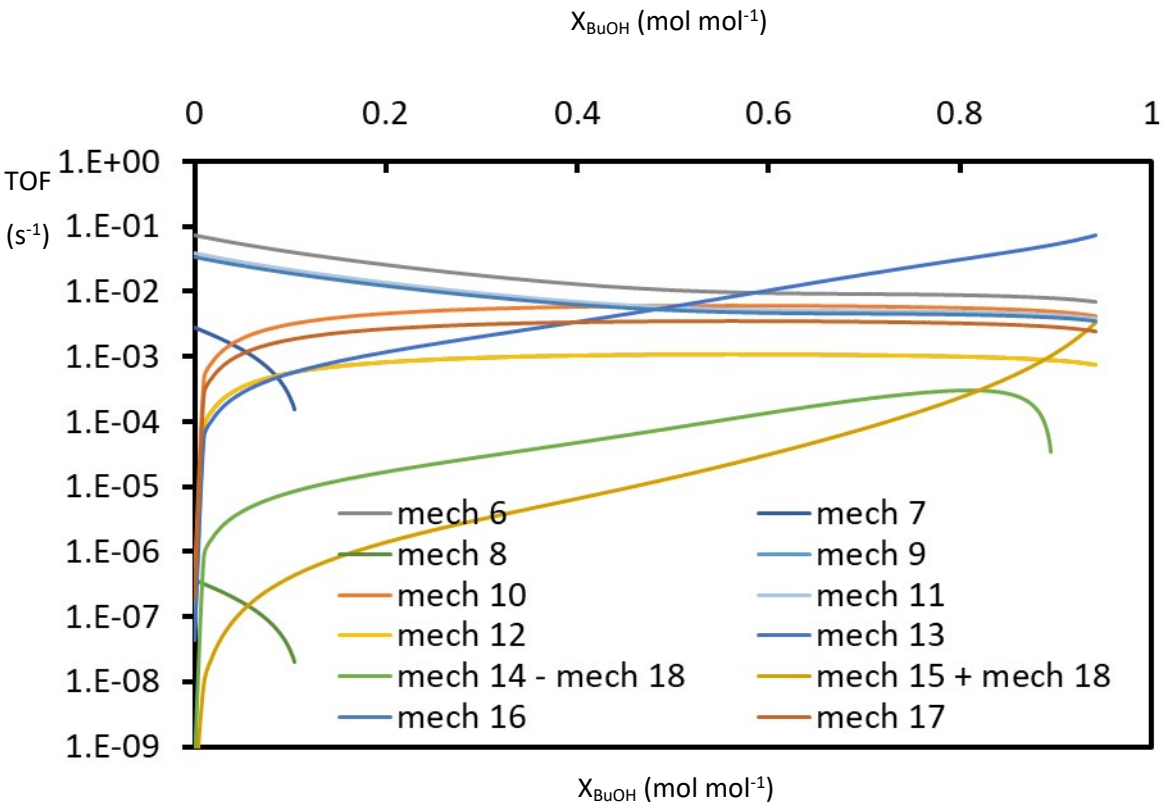

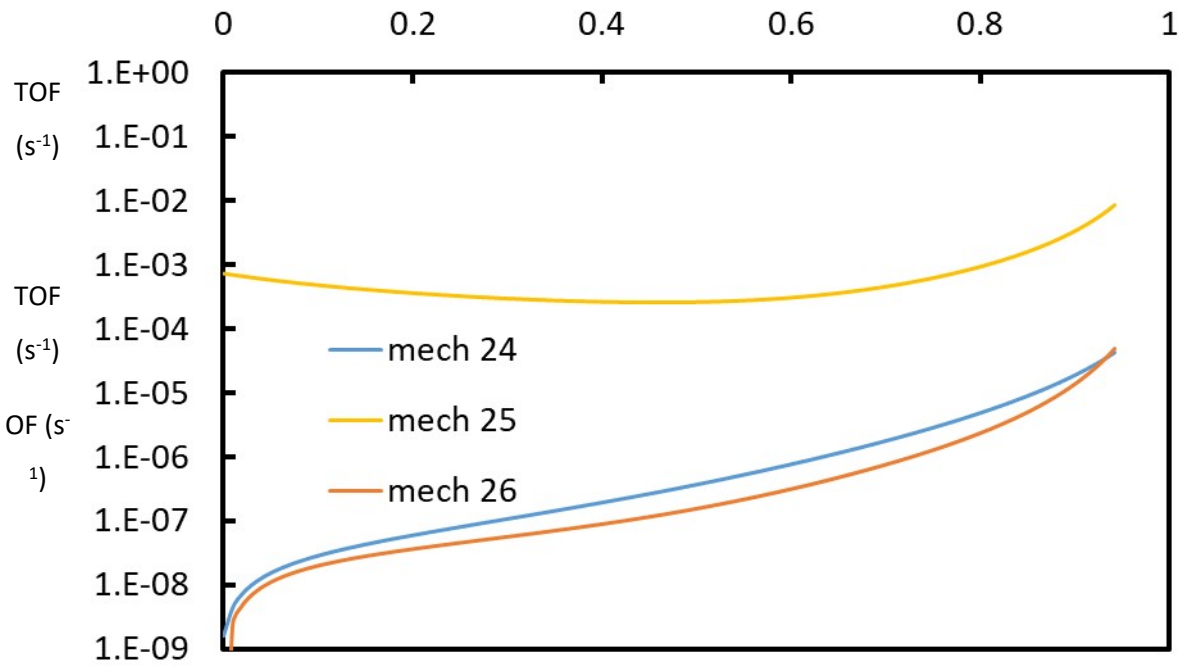

Figure S7. Mechanisms 6 to 26 for the TOFs vs conversion simulations at 500 K. Reaction conditions: temperature = 500 K, p^0_{BuOH} = 29 kPa, p^0_{EtOH} = 7.8 kPa, total pressure = 5 Bar.

These mechanisms 6 to 26 are summarized as follows:

Mechanism 6: dimer-mediated DBE formation ($M1_B$-$D1_{BB}$-$D2_{BB}$-DBE*).

Mechanism 7: Butoxide-mediated S_N2-mechanism DBE formation ($M1_B$-Butoxide-$C3_{BB}$-DBE)

Mechanism 8: Butoxide-mediated S_N1-mechanism DBE formation ($M1_B$-Butoxide-$C3_{BB}$-DBE)

Mechanism 7 and 8 already start at conversion of about 10% to decompose DBE to 2 BuOH molecules. Hence these mechanisms dropping to negative TOFs (not displayed on log scale)

Mechanism 9: Concerted DBE decomposition to 1-butene and DBE (syn-elimination)

Mechanism 10: DBE decomposition through reoriented anti-elimination

Mechanism 11: dimer-mediated trans-2-butene formation ($D1_{BB}$ – trans-2-butene)

Mechanism 12: Concerted DBE decomposition to trans-2-butene

Mechanism 13: Direct 1-butene to trans-2-butene isomerization

Mechanism 14 – mechanism 18: isomerization to trans-2-butene following a butoxide-intermediate (1-butene* - 2-butoxide* - trans-2-butene*). Mechanism 18 is subtracted from 14, as mechanism 18 starts from 2-butene, leads to the butoxide and then reacts towards cis-2-butene (trans-2-butene* -

2-butoxide* - cis-2-butene*). This also explains the decrease of this path near full conversion, as cis-2-butene is then being formed from trans-2-butene.

Mechanism 15 + mechanism 18: isomerization of 1-butene to cis-2-butene (1-butene* - 2-butoxide* - cis-2-butene*), mechanism 18 is added to mechanism 15 as it goes through the same 2-butoxide intermediate to form cis-2-butene (but from trans-butene instead of 1-butene).

Mechanism 16: dimer-mediated cis-2-butene formation ($D1_{BB}$ – cis-2-butene*)

Mechanism 17: Concerted DBE decomposition to cis-2-butene.

Mechanisms 19-23 are discussed in the main text and form ethene from ethanol.

Mechanism 24: Ethoxide-mediated DEE formation ($M1_E$ – Ethoxide – DEE*)

Mechanism 25: Dimer-mediated DEE formation ($M1_E$ – $D1_{EE}$ – $D2_{EE}$ – DEE*)

Mechanism 26: Concerted DEE decomposition to ethene and ethanol.

(S7) Reaction network for n-butanol and ethanol dehydration

The reaction network, consisting of mechanisms 1-18 for n-butanol and 19-26 for ethanol dehydration are summarized in Table S13 and S14.

Table S13. Reaction pathways, mechanisms and elementary steps for n-butanol dehydration in H-ZSM-5 by John et al. [4,5]. Steps that are assumed to be equilibrated are indicated in black, steps for which a transitions state is present are indicated with red stoichiometric numbers (0 means not part of the mechanism).

	Path			**A**				**B**		**C**		**D**	**E**	**F**		**G**	**H**	**I**	**J**
	Mechanism	1	2	3	4	5	6	7	8	9	10	11	12	13	14	15	16	17	18
(R0)	$BuOH_{(g)}$ + * ⇌ $M1_B$	1	1	1	1	0	1	1	1	0	0	0	-1	0	0	0	-1	0	0
(R1)	$M1_B$ ⇌ W + 1-$butene_{(g)}$	1	0	0	0	0	0	0	0	0	0	0	0	0	0	0	0	0	0
(R2)	W ⇌ H_2O(g)	1	1	0	0	0	0	0	0	0	0	0	0	0	0	0	0	0	0
(R3)	M1 ⇌ C1	0	1	0	0	0	0	0	0	0	0	0	0	0	0	0	0	0	0
(R4)	C1 ⇌ W + 1-$butene_{(g)}$	0	1	0	0	0	0	0	0	0	0	0	0	0	0	0	0	0	0
(R5)	$M1_B$ ⇌ $M2_B$	0	0	1	1	0	0	1	1	0	0	0	0	0	0	0	0	0	0
(R6)	$M2_B$ ⇌ 1-butene* + $H_2O_{(g)}$	0	0	1	0	0	0	0	0	0	0	0	0	0	0	0	0	0	0
(R7)	1-butene* ⇌ 1-$butene_{(g)}$ + *	0	0	1	1	0	0	0	0	1	1	0	0	-1	-1	0	0	-1	0
(R8)	$M2_B$ ⇌ Butoxy + $H_2O_{(g)}$	0	0	0	1	0	0	1	1	0	0	0	0	0	0	0	0	0	0
(R9)	butoxy ⇌ 1-butene*	0	0	0	1	0	0	0	0	0	0	0	0	0	0	0	0	0	0
(R10)	$M1_B$ + $BuOH_{(g)}$ ⇌ $D1_{BB}$	0	0	0	0	1	1	0	0	0	0	1	0	0	0	1	0	0	0
(R11)	$D1_{BB}$ ⇌ $D2_{BB}$	0	0	0	0	1	1	0	0	0	0	0	0	0	0	0	0	0	0
(R12)	$D2_{BB}$ ⇌ $C2_B$ + 1-$butene_{(g)}$	0	0	0	0	1	0	0	0	0	0	0	0	0	0	0	0	0	0
(R13)	$C2_B$ ⇌ $M1_B$ + $H_2O_{(g)}$	0	0	0	0	1	0	0	0	0	0	1	0	0	0	1	0	0	0
(R14)	$D2_{BB}$ ⇌ DBE* + $H_2O_{(g)}$	0	0	0	0	0	1	0	0	0	0	0	0	0	0	0	0	0	0
(R15)	DBE* ⇌ $DBE_{(g)}$ + *	0	0	0	0	0	1	1	1	-1	-1	0	-1	0	0	0	-1	0	0
(R16)	Butoxy + $BuOH_{(g)}$ ⇌ $C3_{BB}$	0	0	0	0	0	0	1	1	0	0	0	0	0	0	0	0	0	0
(R17)	$C3_{BB}$ ⇌ DBE* (S_N2)	0	0	0	0	0	0	1	0	0	0	0	0	0	0	0	0	0	0
(R18)	$C3_{BB}$ ⇌ DBE* (S_N1)	0	0	0	0	0	0	0	1	0	0	0	0	0	0	0	0	0	0
(R19)	DBE* ⇌ $C4_{BB}$	0	0	0	0	0	0	0	0	1	0	0	0	0	0	0	0	0	0
(R20)	$C4_{BB}$ ⇌ 1-butene* + $BuOH_{(g)}$	0	0	0	0	0	0	0	0	1	0	0	0	0	0	0	0	0	0
(R21)	DBE* ⇌ DBE2	0	0	0	0	0	0	0	0	0	1	0	0	0	0	0	0	0	0
(R22)	DBE2 ⇌ 1-butene* + $BuOH_{(g)}$	0	0	0	0	0	0	0	0	0	1	0	0	0	0	0	0	0	0
(R23)	$D1_{BB}$ ⇌ $C2_B$ + trans-2-$butene_{(g)}$	0	0	0	0	0	0	0	0	0	0	1	0	0	0	0	0	0	0
(R24)	DBE* ⇌ $M1_B$ + trans-2-$butene_{(g)}$	0	0	0	0	0	0	0	0	0	0	0	1	0	0	0	0	0	0
(R25)	1-butene* ⇌ trans-2-butene*	0	0	0	0	0	0	0	0	0	0	0	0	1	0	0	0	0	0
(R26)	Trans-2-butene*⇌trans-2-$butene_{(g)}$ + *	0	0	0	0	0	0	0	0	0	0	0	0	1	1	0	0	0	-1
(R27)	1-butene* ⇌ 2-Butoxy	0	0	0	0	0	0	0	0	0	0	0	0	0	1	0	0	1	0
(R28)	2-Butoxy ⇌ trans-2-butene*	0	0	0	0	0	0	0	0	0	0	0	0	0	1	0	0	0	-1
(R29)	2-Butoxy ⇌ cis-2-butene*	0	0	0	0	0	0	0	0	0	0	0	0	0	0	0	0	1	1
(R30)	cis-2-butene* ⇌ cis-2-$butene_{(g)}$+ *	0	0	0	0	0	0	0	0	0	0	0	0	0	0	0	0	1	1
(R31)	$D1_{BB}$ ⇌ $C2_B$ + cis-2-$butene_{(g)}$	0	0	0	0	0	0	0	0	0	0	0	0	0	0	1	0	0	0
(R32)	DBE* ⇌ $M1_B$ + cis-2-$butene_{(g)}$	0	0	0	0	0	0	0	0	0	0	0	0	0	0	0	1	0	0

Here W is adsorbed water, C1 is co-adsorbed 1-butene and water, $C2_B$ is co-adsorbed water and n-butanol, $C3_{BB}$ is co-adsorbed n-butanol and butoxy, $C4_{BB}$ is co-adsorbed n-butanol and 1-butene.

Table S14. Reaction pathways, mechanisms and elementary steps for ethanol dehydration in H-ZSM-5 by Alexopoulos et al. [7]. Steps that are assumed to be equilibrated are indicated in black, steps for which a transitions state is present are indicated with red stoichiometric numbers.

	Path			**A**			**B**		**C**
	Mechanism	19	20	21	22	23	24	25	26
(R2)	W ⇌ $H_2O(g)$	1	0	1	0	0	0	0	0
(R33)	$EtOH_{(g)}$ + * ⇌ $M1_E$	1	1	1	0	0	1	1	0
(R34)	$M1_E$ ⇌ $M2_E$	0	1	1	0	0	1	0	0
(R35)	$M2_E$ ⇌ Ethoxy + $H_2O_{(g)}$	0	1	0	0	0	1	0	0
(R36)	Ethoxy -> Ethene*	0	1	0	0	0	0	0	0
(R37)	Ethene* ⇌ $C_2H_{4(g)}$ + *	0	1	0	0	0	0	0	1
(R38)	$M1_E$ + $EtOH_{(g)}$ ⇌ $D1_{EE}$	0	0	0	0	1	0	1	0
(R39)	$D1_{EE}$ ⇌ $D2_{EE}$	0	0	0	0	1	0	1	0
(R40)	$D2_{EE}$ ⇌ DEE* + $H_2O_{(g)}$	0	0	0	0	0	0	1	0
(R41)	DEE* ⇌ $DEE_{(g)}$ + *	0	0	0	0	0	1	1	-1
(R42)	DEE* ⇌ $C1_{EE}$	0	0	0	0	0	0	0	1
(R43)	$C1_{EE}$ ⇌ Ethene* + $EtOH_{(g)}$	0	0	0	0	0	0	0	1
(R44)	Ethoxy + $EtOH_{(g)}$ ⇌ DEE*	0	0	0	0	0	1	0	0
(R45)	$D2_{EE}$ ⇌ $C2_E$ + $C_2H_{4(g)}$	0	0	0	0	1	0	0	0
(R46)	$C2_E$ ⇌ $M1_E$ + $H_2O_{(g)}$	0	0	0	0	1	0	0	0
(R47)	$M1_E$ ⇌ W + $C_2H_{4(g)}$	1	0	0	0	0	0	0	0
(R48)	$M2_E$ ⇌ $C3_E$	0	0	1	0	0	0	0	0
(R49)	$C3_E$ ⇌ W+ $C_2H_{4(g)}$	0	0	1	0	0	0	0	0
(R50)	W +$EtOH_{(g)}$ ⇌ $C2_E$	0	0	0	1	0	0	0	0
(R51)	$C2_E$ ⇌ 2W + $C_2H_{4(g)}$	0	0	0	1	0	0	0	0
(R52)	2W ⇌ W + $H_2O_{(g)}$	0	0	0	1	0	0	0	0

Here $C1_{EE}$ is co-adsorbed ethanol and ethene, $C2_E$ is co-adsorbed co-adsorbed ethanol and water, $C3_E$ is co-adsorbed co-adsorbed ethene and water, 2W is the co-adsorption of 2 water molecules.

[1] C.M. Nguyen, M.F. Reyniers, G.B. Marin, Theoretical study of the adsorption of C1-C4 primary alcohols in H-ZSM-5, Phys Chem Chem Phys, 12 (2010) 9481-9493.
[2] B.A. De Moor, A. Ghysels, M.F. Reyniers, V. Van Speybroeck, M. Waroquier, G.B. Marin, Normal Mode Analysis in Zeolites: Toward an Efficient Calculation of Adsorption Entropies, J Chem Theory Comput, 7 (2011) 1090-1101.
[3] B.A. De Moor, M.F. Reyniers, G.B. Marin, Physisorption and chemisorption of alkanes and alkenes in H-FAU: a combined ab initio-statistical thermodynamics study, Phys Chem Chem Phys, 11 (2009) 2939-2958.
[4] M. John, K. Alexopoulos, M.F. Reyniers, G.B. Marin, Reaction path analysis for 1-butanol dehydration in H-ZSM-5 zeolite: Ab initio and microkinetic modeling, J Catal, 330 (2015) 28-45.
[5] M. John, K. Alexopoulos, M.F. Reyniers, G.B. Marin, Mechanistic insights into the formation of butene isomers from 1-butanol in H-ZSM-5: DFT based microkinetic modelling, Catal Sci Technol, 7 (2017) 1055-1072.

[6] D. Gunst, M. Sabbe, M.-F. Reyniers, A. Verberckmoes, Study of n-butanol conversion to butenes: Effect of Si/Al ratio on activity, selectivity and kinetics, Applied Catalysis A: General, 582 (2019) 117101.
[7] K. Alexopoulos, M. John, K. Van der Borght, V. Galvita, M.-F. Reyniers, G.B. Marin, DFT-based microkinetic modeling of ethanol dehydration in H-ZSM-5, J Catal, 339 (2016) 173-185.
[8] A. de Reviere, D. Gunst, M. Sabbe, A. Verberckmoes, Sustainable short-chain olefin production through simultaneous dehydration of mixtures of 1-butanol and ethanol over HZSM-5 and γ-Al2O3, Journal of Industrial and Engineering Chemistry, 89 (2020) 257-272.
[9] A. de Reviere, T. Vandevyvere, M. Sabbe, A. Verberckmoes, Renewable Butene Production through Dehydration Reactions over Nano-HZSM-5/γ-Al2O3 Hybrid Catalysts, Catalysts, 10 (2020) 879.